Journal of Mechanical Research and Application (JMRA),Vol. 12 No.2, 1401(2022),36-49

Thermoelastic stability of functionally graded ceramic-metal cylindrical shells

M. M. Najafizadeh[a, *], B. Asadi [b], A. H. Nezhadi [a], P. Khazaeinejad [a]

[a] *Department of Mechanical Engineering, Islamic Azad University, Arak Branch, Arak, Iran*
[b] *Department of Basic Sciences, Islamic Azad University, Arak Branch, Arak, Iran*

Abstract

In this paper, the equilibrium and stability equations of a cylindrical shell made of functionally graded material (FGM) under thermal loadings are derived based on the first order and third order shear deformation theories (FSDT and TSDT). Assuming that the material properties vary linearly through the thickness direction and using the variational method, the system of fundamental partial differential equations are established. Then buckling analysis of functionally graded ceramic-metal cylindrical shells under two types of thermal loadings are carried out and the results are given in closed-form solutions. The study concludes that the third order shear deformation theory accurately predicts the behavior of functionally graded ceramic-metal cylindrical shells, whereas the first order shear deformation theory overestimates critical buckling temperatures.

Keywords: Functionally graded material; Ceramic-metal; Cylindrical shells; Thermal buckling

1. Introduction

In recent years studies on new performance materials have addressed new materials known as a functionally graded material (FGM). These are high performance, heat resistant materials able to withstand ultra high temperatures and extremely large thermal gradients used in aerospace industries. FGMs are microscopically inhomogeneous in which the mechanical properties vary smoothly and continuously from one surface to the other [1, 2].

Typically, these materials are made from a mixture of ceramic and metal. It is apparent from the literature survey that most research on FGMs have been restricted to the thermal stress analysis, fracture mechanics, vibration, and optimization. Generally, there are two ways to model the material property gradation in solids: (1) assume a profile for volume fraction [3] and (2) use a micromechanics approach to study the nonhomogeneous media [4].

For composition profile modeling, polynomial representations including quadratic [5] and cubic [6] variations are used. Other representations such as exponential functions [7, 8] and piecewise homogeneous layer representations [9, 10] have also been used. At the micro structural level, an FGM is characterized by transition from a dispersive phase to an alternative structure with a networking structure in between [11]. Specifically Nan et al. [12] used an analytical approach to describe the uncoupled thermomechanical properties of metal/ceramic FGMs. Pindera and Freed [13], Pindera et al. [14] and Aboudi et al. [15] used the unit-cell approach to analyze FGMs. Pindera et al. [16] focused primarily on micromechanics-based studies.

Thermal buckling analysis of isotropic and homogeneous perfect cylindrical shells and composite cylindrical shells based on the Donnell and improved Donnell stability equations are studied by Eslami et al. [17, 18]. Eslami and Shariyat [19] considered the full Green nonlinear strain-displacement relations instead of the simplified Sander's assumption to formulate the dynamic and post buckling of imperfect cylindrical shells. The higher order shear deformation theory, including the normal stress, was used and the mixed formulation was established to simplify the approach of both kinematical and forced boundary conditions. The technique was then improved by the same authors to an exact three-dimensional analysis of circular cylindrical shells based on the equilibrium equations and the full Green nonlinear strain-displacement relations [20]. The Donnell and improved Donnell stability equations are employed to present a closed-form solution for the elastoplastic and creep buckling of cylindrical shells under mechanical loadings at an elevated temperature by Eslami and Shariyat [21]. Eslami and Shahsiah [22] determined the critical thermal buckling of imperfect cylindrical shells.

[*] Corresponding author. Tel./fax: +98 861 367 0084.
Email address: m-najafizadeh@iau-arak.ac.ir (M. M. Najafizadeh).

NOMENCLATURE

R	radius of shell	z	vertical coordinate
h	thickness of shell	x	axial coordinate
E	Young's modulus	θ	circumferential coordinate
N_i	in-plane force	L	lenght of shell
M_i	bending moment	α	coefficient of thermal expansion
u, v, w	axial, circumferential, and transverse displacements, respectively		

They used Donnell and the improved Donnell stability equations and two models for imperfection, namely, the Wan-Donnell and Koiter models. Many post buckling studies based on the classical shell theory of composite laminated thin cylindrical shells subjected to mechanical or thermal loadings or their combinations are available in the literatures, such as Birman and Bert [23] and Shen [24, 25]. Relatively, few studies are available about the application of shear deformation shell theory to post buckling analysis in the literatures, such as those given by Iu and Chia [26] and Reddy and Savoia [27]. In these studies, the material properties are considered independent of temperature. However, studies of temperature and moisture effects on the buckling loads of laminated flat and cylindrical panels are limited in number [28-32], where all these studies assumed perfect initial configuration.

Buckling analysis of FGM structures are rare in the literature. Birman [33] studied the buckling problem of a functionally graded composite rectangular plate subjected to uniaxial compression. The buckling analysis of circular FGM plate is given by Najafizadeh and Eslami [34, 35]. The thermal and mechanical buckling of FGM circular plate based on the first order shear deformation plate theory is studied by Najafizadeh and Hedayati [36]. Javaheri and Eslami [37, 38] presented the mechanical and thermal buckling of a rectangular FGM plates based on the classical and higher order plate theories. Recently, Woo and Meguid [39] gave an analytical solution for large deflection of thin FGM plates and shallow shells. The stabilization of a functionally graded cylindrical shell under axial periodic loading is investigated by Ng et al. [40]. Thermal buckling of functionally graded cylindrical shell based on classical shell theory is studied by Shahsiah and Eslami [41].

In this paper, the thermal buckling analysis of a functionally graded ceramic-metal cylindrical shell is considered. The Donnell nonlinear strain-displacement relations are used. The shell is under uniform temperature rise and radial temperature difference for thermal loading and simply supported boundary conditions are assumed. The expressions for thermal loads are obtained analytically. The results are compared for two shear theories.

2. Derivations

2.1 Material properties

Consider a cylindrical shell made of functionally graded material. The properties of FGMs must be assumed to be graded through the thickness direction. The constituent materials are assumed to be ceramic and metal. The volume fractions of ceramic V_c and metal V_m corresponding to the power law are expressed as [42]

$$V_c = (\frac{2z+h}{2h})^k, \qquad V_m = 1 - V_c \tag{1}$$

where z is the thickness coordinate ($-h/2 \le z \le h/2$), h is the thickness of the shell , and k is the power law index that takes values greater than or equal to zero [42]. In this paper, it is assumed that the properties of FGM shell vary linearly through the thickness direction $(k=1)$. The value of k equal to zero represents a fully ceramic shell. The mechanical and thermal properties of FGMs are determined from the volume fraction of the material constituents. We assumed that the nonhomogeneous material properties such as the modulus of elasticity E and the coefficient of thermal expansion α change in the thickness direction z based on Voigt's rule over the whole range of volume fraction [42]; while Poisson's ratio ν is assumed to be constant [33] as

$$E(z) = E_c V_c + E_m(1-V_c), \qquad \alpha(z) = \alpha_c V_c + \alpha_m(1-V_c), \qquad \upsilon(z) = \upsilon_0 \tag{2}$$

where subscripts m and c refer to the metal and ceramic constituents, respectively. By substituting volume fraction ratio from Eqs. (1) into Eqs. (2), materials properties of the FGM shell is determined, which are the same as proposed by Praveen and Reddy [42]

$$E(z) = E_m + E_{cm}\left(\frac{2z+h}{2h}\right)^k, \qquad \alpha(z) = \alpha_m + \alpha_{cm}\left(\frac{2z+h}{2h}\right)^k, \qquad \upsilon(z) = \upsilon_0 \tag{3}$$

where

$$E_{cm} = E_c - E_m, \qquad \alpha_{cm} = \alpha_c - \alpha_m \tag{4}$$

2.2 Basic equations

Shear deformation theories are those in which the transverse shear stresses are accounted for. Such theories can be used to analyses the mechanical problems with more accuracy. The first order shear deformation theory (FSDT) is the simplest theory that accounts for nonzero transverse shear strains [43]. In the present work, the first order shear deformation theory (FSDT) and the third order shear deformation theory of Reddy (TSDT) are used to obtain the equilibrium and stability equations. The displacement fields based on FSDT and TSDT are [43]

FSDT:

$$\begin{aligned} u(x,\theta,z) &= u_0(x,\theta) + zu_1(x,\theta) \\ v(x,\theta,z) &= v_0(x,\theta) + zv_1(x,\theta) \\ w(x,\theta,z) &= w_0(x,\theta) \end{aligned} \tag{5a}$$

TSDT:

$$\begin{aligned} u(x,\theta,z) &= u_0(x,\theta) + zu_1(x,\theta) - \frac{4z^3}{3h^2}(u_1(x,\theta) + w_{0,x}(x,\theta)) \\ v(x,\theta,z) &= v_0(x,\theta) + zv_1(x,\theta) - \frac{4z^3}{3h^2}(v_1(x,\theta) + w_{0,\theta}(x,\theta)) \\ w(x,\theta,z) &= w_0(x,\theta) \end{aligned} \tag{5b}$$

Here, the z axis is assumed positive outward, u, v, and w denote the displacement components, u_0, v_0, and w_0 denote the displacement in the midsurface of shell (z = 0) and (u_1, v_1) are the rotations of a transverse normal about θ and x axes, respectively, and defined as

$$u_1 = \frac{\partial u}{\partial z}, \qquad v_1 = \frac{\partial v}{\partial z} \tag{6}$$

Consider a thin cylindrical shell of mean radius R and thickness h with length L. The Donnell nonlinear strain-displacement relations are [44]

$$\varepsilon_x = u,x + \frac{1}{2} w,_x{}^2$$
$$\varepsilon_\theta = \frac{v_{,\theta} + w}{R} + \frac{1}{2}(\frac{w_{,\theta}}{R})^2$$
$$\varepsilon_{x\theta} = \frac{u_{,\theta}}{R} + v,x + \frac{w_{,x} w_{,\theta}}{R} \tag{7}$$
$$\varepsilon_{xz} = u_1 + w_{0,x}$$
$$\varepsilon_{\theta z} = v_1 + \frac{w_{0,\theta}}{R}$$

Hook's law for a functionally graded cylindrical shell can be defined as

$$\sigma_x = \frac{E(z)}{(1-\upsilon_0^2)}\left[\varepsilon_x + \upsilon_0 \varepsilon_\theta - (1+\upsilon_0)\alpha T\right]$$
$$\sigma_\theta = \frac{E(z)}{(1-\upsilon_0^2)}\left[\varepsilon_\theta + \upsilon_0 \varepsilon_x - (1+\upsilon_0)\alpha T\right] \tag{8}$$
$$\sigma_{x\theta} = \frac{E(z)}{2(1+\upsilon_0)}\varepsilon_{x\theta}, \qquad \sigma_{\theta z} = \frac{E(z)}{2(1+\upsilon_0)}\varepsilon_{\theta z}, \qquad \sigma_{xz} = \frac{E(z)}{2(1+\upsilon_0)}\varepsilon_{xz}$$

The stress resultants N_i, M_i and Q_i are expressed as

$$(N_i, M_i) = \int_{-\frac{h}{2}}^{\frac{h}{2}} \sigma_i(1, z)\ \mathrm{dz}, \qquad i = x, \theta, x\theta$$
$$Q_j = \int_{-\frac{h}{2}}^{\frac{h}{2}} \sigma_{jz}\ \mathrm{dz}, \qquad j = x, \theta \tag{9}$$

Substituting relations (7) into (8), and the results into Eqs. (9) give the constitutive relations as

FSDT:

$$(N_x, M_x) = \frac{1}{(1-\upsilon_0^2)}\left[(A,B)(\varepsilon_x^0 + \upsilon_0 \varepsilon_\theta^0) + (B,C)(k_x + \upsilon_0 k_\theta) - (1+\upsilon_0)(\mathrm{T}_m, \mathrm{T}_b)\right]$$
$$(N_\theta, M_\theta) = \frac{1}{(1-\upsilon_0^2)}\left[(A,B)(\varepsilon_\theta^0 + \upsilon_0 \varepsilon_x^0) + (B,C)(k_\theta + \upsilon_0 k_x) - (1+\upsilon_0)(\mathrm{T}_m, \mathrm{T}_b)\right]$$
$$(N_{x\theta}, M_{x\theta}) = \frac{1}{2(1+\upsilon_0)}\left[(A,B)(\varepsilon_{x\theta}^0) + (B,C)(k_{x\theta}^0)\right] \tag{10a}$$
$$Q_x = \frac{1}{2(1+\upsilon_0)}\left[A\varepsilon_{xz}^0\right]$$
$$Q_\theta = \frac{1}{2(1+\upsilon_0)}\left[A\varepsilon_{\theta z}^0\right]$$

TSDT:

$$(N_{x_1}, M_{x_1}, P_{x_1}) = \frac{1}{(1-\upsilon_0^2)}\left[(A,B,D)(\varepsilon_{x_1}^0 + \upsilon_0\varepsilon_{\theta_1}^0) + (B,C,F)(k_{x_1} + \upsilon_0 k_{\theta_1}) + (D,F,G)(k_1^1 + \upsilon_0 k_2^1)\right]$$
$$(N_{\theta_1}, M_{\theta_1}, P_{\theta_1}) = \frac{1}{(1-\upsilon_0^2)}\left[(A,B,D)(\varepsilon_{\theta_1}^0 + \upsilon_0\varepsilon_{x_1}^0) + (B,C,F)(k_{\theta_1} + \upsilon_0 k_{x_1}) + (D,F,G)(k_2^1 + \upsilon_0 k_1^1)\right]$$
$$(N_{x\theta_1}, M_{x\theta_1}, P_{x\theta_1}) = \frac{1}{2(1+\upsilon_0)}\left[(A,B,D)\varepsilon_{x\theta_1}^0 + (B,C,F)k_{x\theta_1} + (D,F,G)k_3^1\right] \tag{10b}$$
$$(Q_{x_1}, R_{x_1}) = \frac{1}{2(1+\upsilon_0)}\left[(A,C)\varepsilon_{xz_1}^0 + (C,F)k_{xz_1}\right]$$
$$(Q_{\theta_1}, R_{\theta_1}) = \frac{1}{2(1+\upsilon_0)}\left[(A,C)\varepsilon_{\theta z_1}^0 + (C,F)k_{\theta z_1}\right]$$

where

$$(A,B,C,D,F,G) = \int_{-\frac{h}{2}}^{\frac{h}{2}} (1, z, z^2, z^3, z^4, z^6) E(z) dz \tag{11}$$

The total potential energy V for the cylindrical shell under thermal loading may be written as

$$V = \frac{R}{2}\iiint \left[\sigma_x(\varepsilon_x - \alpha T) + \sigma_\theta(\varepsilon_\theta - \alpha T) + \sigma_{x\theta}\varepsilon_{x\theta} + \sigma_{xz}\varepsilon_{xz} + \sigma_{\theta z}\varepsilon_{\theta z}\right] \mathrm{dx\, d\theta\, dz} \tag{12}$$

where T is the temperature distribution load and function of z. Upon substitution of relations (7) and (8) into Eq. (12), and integrating with respect to z from ($-h/2$ to $h/2$), the total potential energy is obtained as

$$V = \iint F \,\mathrm{dx d\theta} \tag{13}$$

Extremizing the functional of potential energy leads to the Euler equations [44]

$$\frac{\partial F}{\partial u_0} - \frac{\partial}{\partial x}\frac{\partial F}{\partial u_{0,x}} - \frac{\partial}{\partial \theta}\frac{\partial F}{\partial u_{0,\theta}} = 0$$
$$\frac{\partial F}{\partial v_0} - \frac{\partial}{\partial x}\frac{\partial F}{\partial v_{0,x}} - \frac{\partial}{\partial \theta}\frac{\partial F}{\partial v_{0,\theta}} = 0$$
$$\frac{\partial F}{\partial w_0} - \frac{\partial}{\partial x}\frac{\partial F}{\partial w_{0,x}} - \frac{\partial}{\partial \theta}\frac{\partial F}{\partial w_{0,\theta}} + \frac{\partial^2}{\partial x^2}\frac{\partial F}{\partial w_{0,xx}} + \frac{\partial^2}{\partial x \partial \theta}\frac{\partial F}{\partial w_{0,x\theta}} + \frac{\partial^2}{\partial \theta^2}\frac{\partial F}{\partial w_{0,\theta\theta}} = 0 \tag{14}$$
$$\frac{\partial F}{\partial u_1} - \frac{\partial}{\partial x}\frac{\partial F}{\partial u_{1,x}} - \frac{\partial}{\partial \theta}\frac{\partial F}{\partial u_{1,\theta}} = 0$$
$$\frac{\partial F}{\partial v_1} - \frac{\partial}{\partial x}\frac{\partial F}{\partial v_{1,x}} - \frac{\partial}{\partial \theta}\frac{\partial F}{\partial v_{1,\theta}} = 0$$

Substitution of relations (7) and (8) into Eq. (13) and using Eqs. (14), the equilibrium equations for a cylindrical shell composed of functionally graded material are expressed as

FSDT:

$$
\begin{aligned}
&N_{x,x}+\frac{1}{R}N_{x\theta,\theta}=0\\
&N_{x\theta,x}+\frac{1}{R}N_{\theta,\theta}=0\\
&-Q_{x,x}-\frac{1}{R}Q_{\theta,\theta}+(-N_xW_{0,xx}+\frac{-1}{R^2}N_\theta W_{0,\theta\theta}+\frac{-N_{x\theta}}{R}(W_{0,x\theta}+W_{0,x\theta}))+\frac{N_\theta}{R}=0\\
&-M_{x,x}-\frac{1}{R}M_{x\theta,\theta}+Q_x=0\\
&-M_{x\theta,x}-\frac{1}{R}M_{\theta,\theta}+Q_\theta=0
\end{aligned}
\tag{15a}
$$

TSDT:

$$
\begin{aligned}
&N_{x,x}+\frac{1}{R}N_{x\theta,\theta}=0\\
&N_{x\theta,x}+\frac{1}{R}N_{\theta,\theta}=0\\
&-Q_{x,x}-\frac{1}{R}Q_{\theta,\theta}+\frac{4}{h^2}(R_{x,x}+\frac{1}{R}R_{\theta,\theta})-\frac{4}{3h^2}(P_{x,xx}+\frac{1}{R^2}P_{\theta,\theta\theta}+\frac{2}{R}P_{x\theta,x\theta})\\
&-(N_xw_{0,xx}+\frac{1}{R^2}N_\theta w_{0,\theta\theta}+\frac{N_{x\theta}}{R}(w_{0,x\theta}+w_{0,x\theta}))+\frac{N_\theta}{R}=0\\
&-M_{x,x}-\frac{1}{R}M_{x\theta,\theta}+Q_x-\frac{4}{h^2}R_x+\frac{4}{3h^2}(P_{x,x}+\frac{1}{R}P_{x\theta,\theta})=0\\
&-M_{x\theta,x}-\frac{1}{R}M_{\theta,\theta}+Q_\theta-\frac{4}{h^2}R_\theta+\frac{4}{3h^2}(P_{x\theta,x}+\frac{1}{R}P_{\theta,\theta})=0
\end{aligned}
\tag{15b}
$$

The stability equations of cylindrical shell may be derived by the variational approach. If V is the total potential energy of the shell, the first variation δV is associated with the state of equilibrium. The stability of the original configuration of the shell in the neighborhood of the equilibrium state can be determined by the sign of second variation $\delta^2 V$. However, the condition of $\delta^2 V=0$ is used to derive the stability equations of many practical problems on the buckling of shell. Thus, the stability equations are represented by the Euler equations for the integrand in the second variation expression

FSDT:

$$
\begin{aligned}
&N_{x_1,x}+\frac{1}{R}N_{x\theta_1,\theta}=0\\
&N_{x\theta_1,x}+\frac{1}{R}N_{\theta_1,\theta}=0\\
&-Q_{x_1,x}-\frac{1}{R}Q_{\theta_1,\theta}+(-N_{x_0}w^1_{0,xx}+\frac{-1}{R^2}N_{\theta_0}w^1_{0,\theta\theta}+\frac{-N_{x\theta_0}}{R}(w^1_{0,x\theta}+w^1_{0,x\theta}))+\frac{N_{\theta_1}}{R}=0\\
&-M_{x_1,x}-\frac{1}{R}M_{x\theta_1,\theta}+Q_{x_1}=0\\
&-M_{x\theta_1,x}-\frac{1}{R}M_{\theta_1,\theta}+Q_{\theta_1}=0
\end{aligned}
\tag{16a}
$$

TSDT:

$$N_{x_1,x}+\frac{1}{R}N_{x\theta_1,\theta}=0$$
$$N_{x\theta_1,x}+\frac{1}{R}N_{\theta_1,\theta}=0$$
$$-Q_{x_1,x}-\frac{1}{R}Q_{\theta_1,\theta}+\frac{4}{h^2}(R_{x_1,x}+\frac{1}{R}R_{\theta_1,\theta})-\frac{4}{3h^2}(P_{x_1,xx}+\frac{1}{R^2}P_{\theta_1,\theta\theta}+\frac{2}{R}P_{x\theta_1,x\theta})$$
$$-(N_{x_0}w^1_{0,xx}+\frac{1}{R^2}N_{\theta_0}w^1_{0,\theta\theta}+\frac{N_{x\theta_0}}{R}(w^1_{0,x\theta}+w^1_{0,x\theta}))+\frac{N_{\theta_1}}{R}=0 \quad (16b)$$
$$-M_{x_1,x}-\frac{1}{R}M_{x\theta_1,\theta}+Q_{x_1}-\frac{4}{h^2}R_{x_1}+\frac{4}{3h^2}(P_{x_1,x}+\frac{1}{R}P_{x\theta_1,\theta})=0$$
$$-M_{x\theta_1,x}-\frac{1}{R}M_{\theta_1,\theta}+Q_{\theta_1}-\frac{4}{h^2}R_{\theta_1}+\frac{4}{3h^2}(P_{x\theta_1,x}+\frac{1}{R}P_{\theta_1,\theta})=0$$

In Eqs. (16), terms with the subscript 0 are related to the state of equilibrium and terms with the subscript 1 are those characterizing the state of stability. Also, the superscript 1 in the displacement component w_0^1 refers to the state of stability. It is further noticed that while the equilibrium equations are nonlinear, the stability equations are linear. The terms with the subscript 0 are the solution of the equilibrium equation for the given load. The strains and curvatures in terms of displacement components are

$$\varepsilon_{x_0}=u^0_{0,x},\quad \varepsilon_{x_1}=u^1_{0,x},\quad k_{x_0}=u^0_{1,x},\quad k_{x_1}=u^1_1,x$$
$$\varepsilon_{\theta_0}=\frac{v^0_{0,\theta}+w^0_0}{R},\quad \varepsilon_{\theta_1}=\frac{v^1_{0,\theta}+w^1_0}{R},\quad k_{\theta_0}=\frac{v^0_{1,\theta}}{R},\quad k_{\theta_1}=\frac{v^1_{1,\theta}}{R}$$
$$\varepsilon_{x\theta_0}=\frac{u^0_{0,\theta}}{R}+v^0_{0,x},\quad \varepsilon_{x\theta_1}=\frac{u^1_{0,\theta}}{R}+v^1_{0,x},\quad k_{x\theta_0}=\frac{u^0_{1,\theta}}{R}+v^0_{1,x},\quad k_{x\theta_1}=\frac{u^1_{1,\theta}}{R}+v^1_{1,x} \quad (17)$$
$$\varepsilon_{xz_0}=u^0_1+w^0_{0,x},\quad \varepsilon_{xz_1}=u^1_1+w^1_{0,x}$$
$$\varepsilon_{\theta z_0}=v^0_1+\frac{w^0_{0,\theta}}{R},\quad \varepsilon_{\theta z_1}=v^1_1+\frac{w^1_{0,\theta}}{R}$$

Substituting relations (17) into Eqs. (10) and using Eqs. (16), we get the stability equations in terms of the displacement components. These equations are a coupled set of five partial differential equation for the dependent functions u_0, v_0, u_1, v_1 and w_1. They are the Donnell stability equations in coupled form.

3. Buckling analysis

For uniform temperature rise, the initial uniform temperature of the shell is assumed to be T_i. Under simply supported boundary conditions, temperature can be uniformly raised to a final value T_f such that the shell buckles. To find the critical $\Delta T = T_f - T_i$, the prebuckling forces should be found. Solving the membrance from of the equilibrium equations, and using the method developed by Meyers [45] in conjunction with Galerkin's formulation, give the prebuckling force resultants

$$N_{x_0}=-\frac{\Delta T}{(1-\upsilon_0)}(E_m\alpha_m h+\frac{1}{2}E_m\alpha_{cm}h+\frac{1}{2}E_{cm}\alpha_m h+\frac{1}{3}E_{cm}\alpha_{cm}h),\qquad N_{\theta_0}=N_{x\theta_0}=0 \quad (18)$$

For linear temperature variation through the thickness, we approximate a linear temperature variation along the radial direction as

$$T(z)=\frac{\Delta T}{h}(z+\frac{h}{2}) \quad (19)$$

where $\Delta T = T_a - T_b$, T_a is temperature of the inner surface and T_b is temperature of the outer surface of a functionally graded shell. Using the same approach as described for uniform temperature rise, the prebuckling force resultants are

$$N_{x_0} = -\frac{\Delta T}{(1-\upsilon_0)}(E_m\alpha_m h + \frac{1}{3}E_m\alpha_{cm}h + \frac{1}{3}E_{cm}\alpha_m h + \frac{1}{6}E_{cm}\alpha_{cm}h) \quad , \quad N_{\theta_0} = N_{x\theta_0} = 0 \tag{20}$$

The simply supported boundary conditions are defined as [44]

$$v_0^1 = w_0^1 = N_x = M_x = 0 \qquad x = 0, L \tag{21}$$

To solve the system of stability equations, with the consideration of the simply supported boundary conditions (21), the approximate solutions are assumed as

$$\begin{aligned} u_0^1 &= u_0' \cos\lambda x \sin(n\theta) \\ v_0^1 &= v_0' \sin\lambda x \cos(n\theta) \\ w_0^1 &= w_0' \sin\lambda x \sin(n\theta) \qquad & 0 \le x \le L \\ u_1^1 &= u_1' \cos\lambda x \sin(n\theta) \qquad & 0 \le \theta \le 2\pi \\ v_1^1 &= v_1' \sin\lambda x \cos(n\theta) \end{aligned} \tag{22}$$

where $(u_0', v_0', w_0', u_1', v_1')$ are constant coefficients and $\lambda = m\pi / l$, where $m, n = 1,2,3,\ldots$. Substituting relations (22) into the stability equations (16), yield a system of five homogeneous equations for $(u_0', v_0', w_0', u_1', v_1')$ that is,

$$\begin{bmatrix} K_{11} & K_{12} & K_{13} & K_{14} & K_{15} \\ K_{21} & K_{22} & K_{23} & K_{24} & K_{25} \\ K_{31} & K_{32} & K_{33} & K_{34} & K_{35} \\ K_{41} & K_{42} & K_{43} & K_{44} & K_{45} \\ K_{51} & K_{52} & K_{53} & K_{54} & K_{55} \end{bmatrix} \begin{bmatrix} u_0' \\ v_0' \\ w_0' \\ u_1' \\ v_1' \end{bmatrix} = \begin{bmatrix} 0 \\ 0 \\ 0 \\ 0 \\ 0 \end{bmatrix} \tag{23}$$

In which K_{ij} is a symmetric matrix with the components (The values of K_{ij} for the case of FSDT and TSDT are listed in Appendix). Substituting prebuckling forces from Eqs. (18) and (20) into the relations of K_{ij} and setting $|K_{ij}|=0$ to obtain the nonzero solution, the value of ΔT are found for uniform and linear radial temperature rises. The critical buckling temperature is obtained by minimizing ΔT with respect to m and n, the number of longitudinal and circumferential buckling waves.

4. Results and discussion

A functionally graded ceramic-metal cylindrical shell is considered. The combination of materials consists of steel and alumina. The Young҆s modulus for steel and alumina are: $E_m = 200GPa, \alpha_m = 11.7\times10^{-6} /^0 C$ and $E_c = 380GPa$, $\alpha_C = 7.4\times10^{-6} /^0 C$, respectively. The Poisson's ratio is chosen to be 0.3 for steel and alumina. The boundary conditions are assumed to be simply supported.

Comparisons of the critical buckling temperatures based on the first order and third order shear deformation theories (FSDT and TSDT) for the two types of thermal loadings with respect to radius of shell R are presented in Tables 1 and 2. These Tables show that the critical buckling temperature decreases by the increasing of the radius R (for $L/R = 0.5$) and by decreasing the shell thickness.

Tables 3 and 4 show the results of the critical buckling temperature for the critical uniform and linear radial temperature rise relative to L/R and h/R for a constant value of radius. Also, these Tables show that the critical buckling temperature increases by the increasing of the thickness-to-radius ratio h/R and by the decreasing of the L/R.

To illustrate the effects of radius, the ratios h/R, and and L/R, the variation of the critical temperature difference ΔT_{cr} versus variation of the dimensionless geometrical parameter h/R and R are plotted for two loading cases based on first and third order shear deformation plate theories in Figs. 1-4.

Table 1.
Variation of the critical uniform temperature rise due to FSDT and TSDT with respect to R ($L/R=0.5$)

h (m)		$R=0.625$ m	$R=0.875$ m	$R=1.25$ m	$R=1.75$ m	$R=2$ m
0.007	FSDT	504.666	361.685	249.972	180.697	156.235
	TSDT	498.967	356.487	245.334	177.409	156.200
0.005	FSDT	361.685	255.355	180.697	129.770	111.768
	TSDT	356.487	251.669	177.545	127.586	110.865
0.003	FSDT	215.290	153.004	107.154	76.559	67.467
	TSDT	213.836	152.966	107.136	76.549	67.464

Table 2.
Variation of the critical linear radial temperature rise due to FSDT and TSDT with respect to R ($L/R=0.5$)

h (m)		$R=0.625$ m	$R=0.875$ m	$R=1.25$ m	$R=1.75$ m	$R=2$ m
0.007	FSDT	1039.565	745.037	514.919	372.218	321.830
	TSDT	1030.697	738.726	513.605	365.447	321.758
0.005	FSDT	745.037	526.007	372.218	266.819	230.132
	TSDT	734.329	524.594	365.447	261.441	229.983
0.003	FSDT	443.478	315.174	220.727	157.706	138.976
	TSDT	439.856	315.096	220.691	157.685	138.971

Table 3.
Variation of the critical uniform temperature rise due FSDT and TSDT with respect to h/R ($R=0.5$ m)

L/R		$h/R=0.001$	$h/R=0.003$	$h/R=0.005$	$h/R=0.008$	$h/R=0.01$
1.9	FSDT	44.668	99.437	180.636	334.145	448.056
	TSDT	44.664	98.174	177.090	327.677	437.891
0.8	FSDT	44.690	104.673	191.158	352.520	480.839
	TSDT	44.980	103.055	186.176	345.397	469.414
0.3	FSDT	45.598	110.906	200.798	376.213	516.580
	TSDT	45.435	108.753	195.674	368.344	504.386

Table 4.
Variation of the critical linear radial temperature rise due to FSDT and TSDT with respect to h/R ($R=0.5$ m)

L/R		$h/R=0.001$	$h/R=0.003$	$h/R=0.005$	$h/R=0.008$	$h/R=0.01$
1.9	FSDT	92.011	200.186	359.406	663.342	885.297
	TSDT	92.007	198.598	355.901	657.627	877.348
0.8	FSDT	92.057	211.583	372.174	680.718	910.768
	TSDT	92.032	208.610	368.253	674.253	901.753
0.3	FSDT	92.201	223.368	388.225	704.358	939.673
	TSDT	93.105	219.647	383.735	696.762	930.142

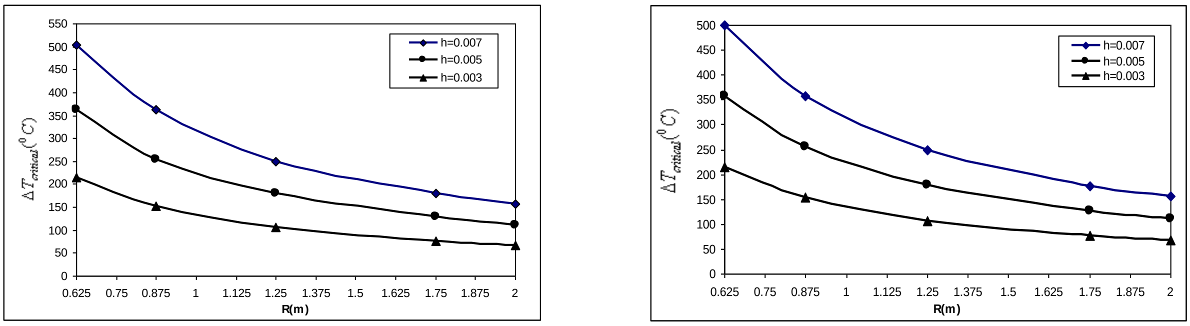

(a) **(b)**

Fig. 1. Critical uniform temperature rise versus the radius R ($L/R = 0.5$); (a): FSDT, (b): TSDT.

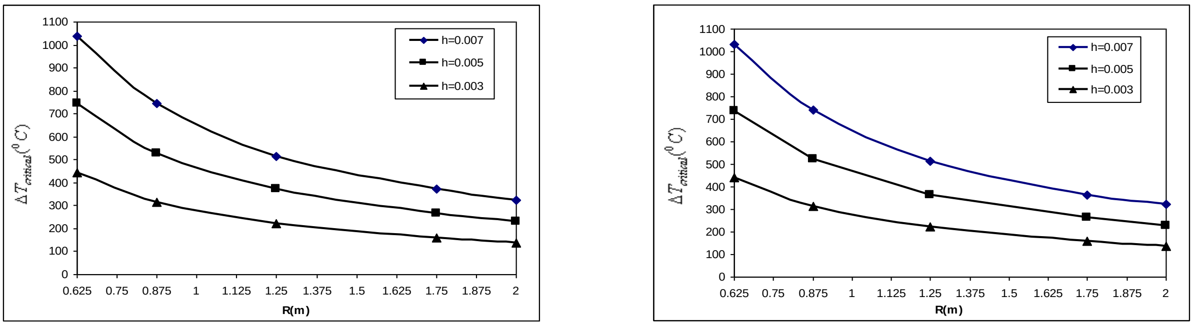

(a) **(b)**

Fig. 2. Critical linear radial temperature rise versus the radius R ($L/R = 0.5$); (a): FSDT, (b): TSDT.

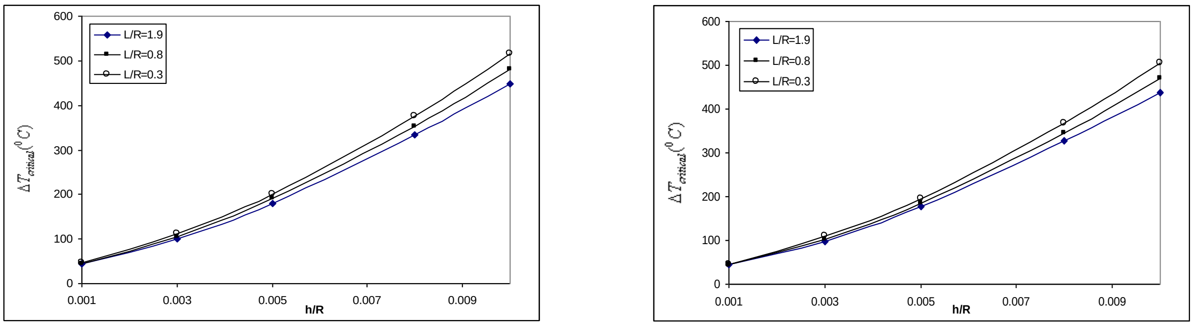

(a) **(b)**

Fig. 3. Critical uniform temperature rise versus the ratio h/R ($R = 0.5$ m); (a): FSDT, (b): TSDT.

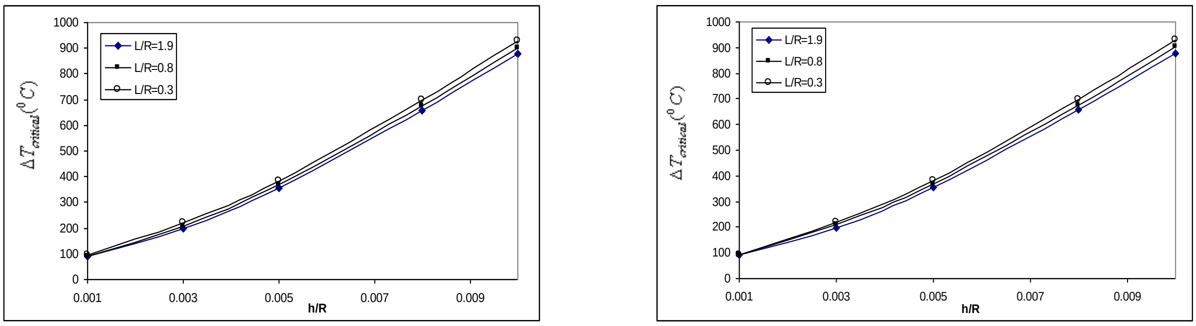

(a) **(b)**

Fig. 4. Critical linear radial temperature rise versus the ratio h/R ($R=0.5$ m); (a): FSDT, (b): TSDT.

5. Conclusions

In the present paper, equilibrium and stability equations for simply supported functionally graded cylindrical shells are obtained. Derivations are based on the first order and third order shear deformation theories (FSDT and TSDT) with the assumption of linear composition for the material. Then, the buckling analysis of functionally graded ceramic-metal cylindrical shells under two different thermal loading cases is investigated. It is concluded that:

1. The third order shear deformation theory (TSDT) underestimates the buckling loads compared with the first order shear deformation theory (FSDT). Critical buckling loads predicted by the two theories are very close to each other.
2. The critical temperature difference ΔT_{cr} is increased with an increase of the ratio h/R.
3. The critical temperature difference ΔT_{cr} for the functionally graded cylindrical shell under linear temperature difference through the thickness is twice that of the functionally graded cylindrical shell under initial-final temperature difference.
4. The critical temperature difference ΔT_{cr} is decreased with an increase of the radius R.
5. The critical temperature difference ΔT_{cr} is increased with an decrease of the ratio L/R.

Appendix :

The values of K_{ij} for the case of FSDT and TSDT

The values of K_{ij} for the case of FSDT:

$$K_{11}=A(\frac{\lambda^2}{(1-\upsilon_0)}+\frac{n^2}{2R^2})$$

$$K_{12}=A(\frac{\upsilon_0\lambda n}{R(1-\upsilon_0)}+\frac{\lambda n}{2R})$$

$$K_{13}=\frac{-A\upsilon_0\lambda}{R(1-\upsilon_0)}$$

$$K_{14}=0,\quad K_{15}=0$$

$$K_{22}=A(\frac{n^2}{R^2(1-\upsilon_0)}+\frac{\lambda^2}{2})$$

$$K_{23}=\frac{-An}{R^2(1-\upsilon_0)}$$

$$K_{24}=0,\quad K_{25}=0$$

$$K_{33}=A(\frac{\lambda^2}{2}+\frac{n^2}{2R^2}+\frac{1}{R^2(1-\upsilon_0)})+\frac{N_{\theta_0}n^2(1+\upsilon_0)}{R^2}$$

$$K_{34}=\frac{A\lambda}{2},\quad K_{35}=\frac{An}{2R}$$

$$K_{44}=\frac{A}{2}+C(\frac{\lambda^2}{(1-\upsilon_0)}+\frac{n^2}{2R^2})$$

$$K_{45}=C(\frac{\upsilon_0\lambda n}{R(1-\upsilon_0)}+\frac{n\lambda}{2R})$$

$$K_{55}=\frac{A}{2}+C(\frac{\lambda^2}{2}+\frac{n^2}{R^2(1-\upsilon_0)})$$

The values of K_{ij} for the case of TSDT:

$$K_{11}=A\left(\frac{\lambda^2}{(1-\upsilon_0)}+\frac{n^2}{2R^2}\right)$$

$$K_{12}=A\left(\frac{\upsilon_0\lambda n}{R(1-\upsilon_0)}+\frac{\lambda n}{2R}\right)$$

$$K_{13}=\frac{-A\upsilon_0\lambda}{R(1-\upsilon_0)}-D\left(\frac{4\lambda^3}{3h^2(1-\upsilon_0)}+\frac{4\upsilon_0 n^2\lambda}{3h^2R^2(1-\upsilon_0)}+\frac{4n^2\lambda}{3h^2R^2}\right)$$

$$K_{14}=B\left(\frac{\lambda^2}{(1-\upsilon_0)}+\frac{n^2}{2R^2}\right)-D\left(\frac{4\lambda^2}{3h^2(1-\upsilon_0)}+\frac{2n^2}{3h^2R^2}\right)$$

$$K_{15}=B\left(\frac{\upsilon_0\lambda n}{R(1-\upsilon_0)}+\frac{\lambda n}{2R}\right)-D\left(\frac{4\upsilon_0\lambda n}{3h^2R(1-\upsilon_0)}+\frac{2\lambda n}{3h^2R}\right)$$

$$K_{22}=A\left(\frac{n^2}{R^2(1-\upsilon_0)}+\frac{\lambda}{2}\right)$$

$$K_{23}=-A\left(\frac{n}{R^2(1-\upsilon_0)}\right)-4D\left(\frac{n^3}{3h^2R^3(1-\upsilon_0)}+\frac{\upsilon_0\lambda^2 n}{3h^2R(1-\upsilon_0)}+\frac{\lambda^2 n}{3h^2R}\right)$$

$$K_{24}=B\left(\frac{\lambda n}{2R}+\frac{\upsilon_0\lambda n}{R(1-\upsilon_0)}\right)-2D\left(\frac{2\upsilon_0\lambda n}{3h^2R(1-\upsilon_0)}+\frac{\lambda n}{3h^2R}\right)$$

$$K_{25}=B\left(\frac{\lambda^2}{2}+\frac{n^2}{R^2(1-\upsilon_0)}\right)-2D\left(\frac{2n^2}{3h^2R^2(1-\upsilon_0)}+\frac{\lambda^2}{3h^2}\right)$$

$$K_{33}=A\left(\frac{\lambda^2}{2}+\frac{n^2}{2R^2}+\frac{1}{R^2(1-\upsilon_0)}\right)-4C\left(\frac{\lambda^2}{h^2}+\frac{n^2}{h^2R^2}\right)+$$

$$8D\left(\frac{\upsilon_0\lambda^2}{3Rh^2(1-\upsilon_0)}+\frac{n^2}{3h^2R^3(1-\upsilon_0)}\right)+8F\left(\frac{\lambda^2}{h^4}+\frac{n^2}{R^2h^4}\right)$$

$$+16G\left(\frac{\lambda^4}{9h^2(1-\upsilon_0)}+\frac{\upsilon_0\lambda^2n^2}{9h^4R^2(1-\upsilon_0)}+\frac{n^4}{9h^4R^4(1-\upsilon_0)}+\frac{\upsilon_0\lambda^2n^2}{9h^4R^2(1-\upsilon_0)}+\frac{2\lambda^2n^2}{9h^4R^2}\right)$$

$$+\left(N_{x_0}\lambda^2+\frac{1}{R^2}N_{\theta_0}n^2+\frac{-N_{x\theta_0}\lambda n(R+1)}{R}\right)(1+\upsilon_0)$$

$$K_{34}=A\left(\frac{\lambda}{2}\right)-\frac{B\upsilon_0\lambda}{R(1-\upsilon_0)}-\frac{4C\lambda}{h^2}+\frac{4D\upsilon_0\lambda}{3Rh^2(1-\upsilon_0)}-4F\left(\frac{\lambda^3}{3h^2(1-\upsilon_0)}+\frac{\upsilon_0\lambda n^2}{3h^2R^2(1-\upsilon_0)}+\frac{\lambda n^2}{3h^2R^2}-\frac{2\lambda}{h^4}\right)$$
$$+16G\left(\frac{\lambda^3}{9h^4(1-\upsilon_0)}+\frac{\upsilon_0\lambda n^2}{9h^4R^2(1-\upsilon_0)}+\frac{\lambda n^2}{9h^4R^2}\right)$$

$$K_{35}=\frac{An}{2R}-\frac{Bn}{R^2(1-\upsilon_0)}-\frac{4Cn}{Rh^2}+\frac{4Dn}{3h^2R^2(1-\upsilon_0)}-4F\left(\frac{n^3}{3h^2R^3(1-\upsilon_0)}+\frac{\lambda^2 n}{3Rh^2}+\frac{\upsilon_0\lambda^2 n}{3Rh^2(1-\upsilon_0)}-\frac{2n}{h^4R}\right)$$
$$+16G\left(\frac{\upsilon_0\lambda^2 n}{9h^4R(1-\upsilon_0)}+\frac{n^3}{9h^4R^3(1-\upsilon_0)}+\frac{\lambda^2 n}{9h^4R}\right)$$

$$K_{44}=\frac{A}{2}+C\left(\frac{\lambda^2}{(1-\upsilon_0)}+\frac{n^2}{2R^2}-\frac{4}{h^2}\right)+4F\left(\frac{-2\lambda^2}{3h^2(1-\upsilon_0)}-\frac{n^2}{3h^2R^2}+\frac{2}{h^4}\right)+16G\left(\frac{\lambda^2}{9h^4(1-\upsilon_0)}+\frac{n^2}{18h^4R^2}\right)$$

$$K_{45}=C\left(\frac{\upsilon_0 n\lambda}{R(1-\upsilon_0)}+\frac{n\lambda}{2R}\right)-4F\left(\frac{2\upsilon_0 n\lambda}{3Rh^2(1-\upsilon_0)}+\frac{n\lambda}{3Rh^2}\right)+16G\left(\frac{\upsilon_0 n\lambda}{9Rh^4(1-\upsilon_0)}+\frac{n\lambda}{18Rh^4}\right)$$

$$K_{55}=\frac{A}{2}+C\left(\frac{\lambda^2}{2}+\frac{n^2}{R^2(1-\upsilon_0)}-\frac{4}{h^2}\right)-4F\left(\frac{\lambda^2}{3h^2}+\frac{2n^2}{3h^2R^2(1-\upsilon_0)}-\frac{2}{h^4}\right)+16G\left(\frac{\lambda^2}{18h^4}+\frac{n^2}{9R^2h^4(1-\upsilon_0)}\right)$$

REFFERENCES

[1] Suresh, S., Mortensen, A.: Fundamentals of functionally graded materials. Barnes and Noble Pub.: London 1998.

[2] Yamanouchi, M., Koizumi, M., Shiota I.: Proceeding of the first international symposium on functionally gradient materials. Sendai: Japan 1990.

[3] Fukui, Y.: Fundamental investigation of functionally gradient material manufacturing system using centrifugal force. Int. J. Jpn. Soc. Mech. Eng. **3**, 144 -148 (1991).

[4] Reddy, J. N., Cheng, Z. Q.: Three dimensional trenchant deformations of functionally graded rectangular plates. Eur. J. Mech. A/ Solids **20**, 841-855 (2001).

[5] Fuchiyama, T., Noda, N., Tsuji, T., Obata, Y.: Analysis of thermal stress and stress intensity factor of functionally gradient materials. Ceramic Trans., Functionally gradient materials **34**, 425-432 (1993).

[6] Williamson, R. L., Rabin, B. H., Drake, J. T.: Finite element analysis of thermal residual stresses at graded ceramic-metal interfaces, Part 1, model description and geometric effects. Appl. Phys. J. **74**, 1310-1320 (1993).

[7] Delale, F., Erdogan, F.: The crack problem for a nonhomogeneous plane. J. Appl. Mech. (Trans. ASME) **50**, 609-614 (1983).

[8] Noda, N., Jin, Z. H.: Thermal stress intensity factors for a crack in a strip of a functionally gradient material. Int. J. Solids Struct. **30**, 1039-1056 (1993).

[9] Araki N., Makino, A., Ishiguro, T., Mihara, J.: An analytical solution of temperature response in multilayered material for transient method. Int. J. Thermophys. **13**, 515-538 (1992).

[10] Tanigawa, Y.: Theoretical approach of optimum design for a plate of functionally gradient materials under thermal loading, thermal shock and thermal fatigue behavior of advanced ceramics. NATO ASI Ser. E **241**, 171-180 (1992).

[11] Zhai, P. C., Jiang, C. R., Zhang, Q. I.: Application of three-Phase micromechanical theories to ceramic/metal functionally gradient materials. Ceramic Trans., Functionally Gradient Materials **34**, 441-449 (1993).

[12] Nan, C. W., Yuan, R. Z., Zhang, L. M.: The physics of metal/ceramic functionally gradient materials. Ceramic Trans., Functionally gradient materials **34**, 75-82 (1993).

[13] Pindera, M. J., Freed, A. D.: The effect of matrix microstructure on the evolution or residual stresses in titanium-aluminie composites AMD. ASME **40**, 37-52, New York (1992).

[14] Pindera, M. J., Salzar, R. S., Williams, T. O.: An evaluation of a new approach for the thermo-plastic response of metal-mtrix composites. Compos. Eng. **3**, 1185-1201 (1993).

[15] Aboudi, J., Pindera, M. J., Arnold, S. M.: Thermoelastic response of metal matrix composites with large diameter fibers subjected to thermal gradients. NASA Technical Memorandum 106-344. Springfield: VA (1993).

[16] Pindera, M. J., Arnold, S. M., Aboudi, J., Hui, D.: Use of composites in functionally gradient materials. Compos. Eng. (1994).

[17] Eslami, M. R., Ziaii, A. R., Ghorbanpour, A.: Thermoelastic buckling of thin cylindrical shells based on improved donnell equations. J. Thermal Stresses **19**, 299-316 (1996).

[18] Eslami, M. R., Javaheri, R.: Thermal and mechanical buckling of composite cylindrical shells. J. Thermal Stresses **22**, **(**6): 527-545 (1999).

[19] Eslami, M. R., Shariyat, M.: A high-order theory for dynamic buckling and post buckling analysis of laminated cylindrical shell. J. Pressure Vessel Tech. (Trans. ASME) **121**, 94-102, February (1999).

[20] Eslami, M. R., Shariyat, M.: Dynamic buckling and post buckling of imperfect orthotropic cylindrical shells under mechanical and thermal loads, based on the three-dimensional theory of elasticity. J. Appl. Mech. (Trans. ASME) **6**, 475-484, June (1999).

[21] Eslami, M. R., Shariyat, M.: elastic, plastic and creep buckling of imperfect cylinders under mechanical and thermal loading. J. Pressure Vessel Tech. (Trans. ASME) **118**, (1996).

[22] Eslami, M. R., Shahsiah, R.: Thermal buckling of imperfect cylindrical shells. J. Thermal Stresses **24**, 71-90 (2000).

[23] Birman, V., Bert, C. W.: Buckling and post buckling of composite plates and shells subjected to elevated temperature. J. Appl. Mech (Trans. ASME) **60**, 514-519 (1993).

[24] Shen, H. S.: Post buckling analysis of imperfect stiffened laminated cylindrical shells under combined external pressure and axial compression. Comput. Struct. **63**, 335-348 (1997).

[25] Shen, H. S.: Thermo Mechanical post buckling of composite laminated cylindrical shells with local geometric imperfections. Int. J. Solids Struct. **36**, 597-617 (1999).

[26] Iu, V. P., Chia, C. Y.: Effect of transverse shear on nonlinear vibration and post buckling of an symmetric cross-ply imperfect Cylindrical shells. Int. J. Mech. Sci. **30**, 705- 718 (1988).

[27] Reddy, J. N., Savoia, M.: Layer-Wise shell theory for post buckling of laminated circular cylindrical shells. AJAA J. **30**, 2148-2154 (1992).

[28] Whitney, J. M., Ashton, J. E.: Effect of environment on the elastic response of layered composite plates. AIAA J. **9**, 1705-1713 (1971).

[29] Snead, J. M., Palazotto, A. N.: Moisture and temperature effects on the instability of cylindrical composite panels. J. Aircraft **20**, 777-783 (1983).

[30] Lee, S. Y., Yen, W. J.: Hydrothermal effects on the stability of a cylindrical composite shell panel. Comput. Struct. **33**, 551-559 (1989).

[31] Ram, K. S. S., Sinha, P. K.: Hydrothermal effects on the buckling of laminated composite plates. Compos. Struct. **21**, 233-247 (1992).

[32] Chao, L. P., Shyu, S. L.: Nonlinear budding of fiber reinforced composite plates under hydrothermal effects. J. Chinese Inst. Eng. **19**, 657-667 (1996).

[33] Birman, V.: Buckling of functionally graded hybrid composite plates. Proceeding of the 10th conference on engineering mechanics **2**, 1199-1202 (1995).

[34] Najafizadeh, M. M., Eslami, M. R.: Buckling analysis of circular plates of functionally graded materials under uniform redial compression. J. Mech. Sci. **4**, 2479-2493 (2002a).

[35] Najafizadeh, M. M., Eslami, M. R.: First-order-theory-based thermoelastic stability of functionally graded material circular plates. AIAA J. **40**, 1444-1450 (2002b).

[36] Najafizadeh, M. M., Hedayati, B.: Refined theory for thermoelastic stability of functionally graded circular plates. J. Thermal Stresses **27**, 857-880 (2004).

[37] Javaheri, R., Eslami, M. R.: Buckling of functionally graded plates under in-plane compressive loading. ZAMM J. **82**, 277-283 (2002).

[38] Javaheri, R., Eslami, M. R.: Thermal buckling of functionally graded plates based on higher order theory. J. Thermal Stresses **25**, 603-625 (2002).

[39] Woo, J., Meguid, S. A.: Nonlinear analysis of functionally graded plates and shallow shells. Int. J. Solids Struct. **38**, 7409-7421 (2001).

[40] Ng, T. Y., Lam, Y. K., Liew, K. M., Reddy, J. N.: Dynamic stability analysis of functionally graded cylindrical shell under periodic axial loading. Int. J. Solids Struct. **38**, 1295-1300 (2001).

[41] Shahsiah, R., Eslami, M. R.: Thermal buckling of functionally graded cylindrical shell. J. Thermal Stresses **26**, 277-294 (2003).

[42] Praveen, G. N., Reddy, J. N.: Nonlinear transient thermoelastic analysis of functionally graded ceramic metal plates. Int. J. Solids Struct. **35**, 4457-4471 (1998).
[43] Reddy, J. N., Khdeir, A. A.: Buckling and vibration of laminated composite plates using various plate theories. AIAA J. **27**, 1808-1817 (1989).
[44] Brush, D. O., Almorth, B. O,: Buckling of bars, plate and shells. McGraw- Hill: New York (1975).
[45] Meyers C. A., Hyer, M. W.: Thermal buckling and post buckling of symmetrically laminated composite plates. J. Thermal Stresses **14**, 519-540 (1991).